Inward dispersion of the spin excitation spectrum of stripe-ordered $La_2NiO_{4+\delta}$

P. G. Freeman and M. Enderle
Institut Laue-Langevin, BP 156, 38042 Grenoble Cedex 9, France

S. M. Hayden
H. H. Wills Physics Laboratory, University of Bristol, Bristol BS8 1TL, United Kingdom

C. D. Frost
ISIS Facility, Rutherford Appleton Laboratory, Chilton, Didcot OX11 0QX, United Kingdom

D. X. Yao and E. W. Carlson
Department of Physics, Purdue University, West Lafayette, Indiana 47907, USA

D. Prabhakaran and A. T. Boothroyd*
Department of Physics, Oxford University, Oxford OX1 3PU, United Kingdom
(Received 29 September 2009; published 23 October 2009)

Polarized- and unpolarized-neutron scattering measurements of the spin excitation spectrum in the stripe-ordered phase of $La_2NiO_{4+\delta}$ ($\delta \simeq 0.11$) are presented. At low energies, the magnetic spectral weight is found to shift anomalously toward the two-dimensional antiferromagnetic wave vector, similar to the low-energy dispersions observed in cuprate superconductors. While spin-wave spectra in stripe phases can exhibit an apparent inward dispersion, we find that the peak shifts measured here cannot be accounted for by this effect. Possible extensions of the model are discussed.

DOI: 10.1103/PhysRevB.80.144523 PACS number(s): 75.30.Ds, 71.45.Lr, 75.30.Fv, 75.30.Et

I. INTRODUCTION

Nanoperiodic spin and charge correlations in the form of stripes have featured prominently in the debate over the mechanism of superconductivity in the layered cuprates.[1] Of particular interest has been the interpretation of the spin fluctuation spectrum measured by neutron scattering, which exhibits a characteristic hour-glass shape in hole-doped cuprates.[2–11] The hour-glass dispersion is found in cuprates both with and without static stripe order, and has recently been observed[11] in a very lightly doped insulating cuprate in which the incommensurate spin modulation is diagonal, i.e., at 45° to the Cu–O bonds, rather than parallel to the bonds as found at higher doping. Theoretical approaches based on stripes[12–18] generally succeed in reproducing the gross features of the spectrum, but the low-energy part remains a concern.[19] These models invariably predict cones of spin excitations emerging from four equivalent incommensurate (IC) wave vectors (two in the case of untwinned unidirectional stripes). Such spin-wave cones, however, are not observed experimentally in the cuprates. Instead, the spectra show four IC peaks that disperse inwards with energy *without splitting* toward the ordering wave vector $\mathbf{Q}_{AF}$ of the parent antiferromagnet where they merge before dispersing apart again at higher energies.

Insight into the role of stripes in the cuprates can be gained from the structurally related but insulating system $La_{2-x}Sr_xNiO_{4+\delta}$, whose phase diagram exhibits stable stripe order over a wide range of hole content $n_h = x + 2\delta$ without the complication of superconductivity.[20–25] Stripes in $La_{2-x}Sr_xNiO_{4+\delta}$ are aligned at 45° to the Ni–O bonds, like in lightly doped $La_{2-x}Sr_xCuO_4$, but as noted above, the characteristic features of the magnetic dispersion in the cuprates is not dependent on the alignment of the stripes. Detailed measurements of $La_{2-x}Sr_xNiO_{4+\delta}$ have been reported for several compositions close to $x = 1/3$ with $\delta = 0$.[26–29] Like in the cuprates, the low-energy spectra show four IC peaks, but so far no evidence has been found for an inward dispersion. With the exception of an unexplained peak near 25 meV,[27,28] the spectra are consistent with propagating spin-wave modes of ordered stripes.

In this paper, we report neutron scattering measurements of the spin excitation spectrum of $La_2NiO_{4.11}$. Previous studies of the spin excitations in the nickelates have mostly been performed on compounds whose stripe period is 1.5 to 2 times shorter than found in stripe-ordered cuprates. In $La_2NiO_{4.11}$, however, the stripe period is similar to that in the cuprates. Oxygen-doped $La_2NiO_{4+\delta}$ exhibits stripe order for $\delta \gtrsim 0.11 (n_h \gtrsim 0.22)$.[23,24] For $0 \leq \delta \lesssim 0.11$, commensurate antiferromagnetic (AFM) order of the parent phase ($\delta = 0$) is observed but with an ordering temperature that decreases with δ. The advantage of O doping over Sr doping is that for a given hole concentration there is less disorder in the stripes, possibly as a result of three-dimensional ordering of the interstitial oxygen combined with a lack of cation disorder.

Our measurements reveal an anomalous inward dispersion of the spectral weight in the energy range 10 to 25 meV, while above ~25 meV, the IC peaks are found to split into spin-wave cones. This shows that the magnetic excitations of a stripe-ordered antiferromagnet can display similar behavior at low energies to that found in the hole-doped cuprates, although in $La_2NiO_{4+\delta}$ the complete hour-glass dispersion is not observed. Our attempts to model the results quantitatively suggest that a description that goes beyond linear spin-wave theory for ideal stripes is required.

II. EXPERIMENTAL DETAILS

The single crystal of $La_2NiO_{4+\delta}$ used here was grown in Oxford by the floating-zone method[30] and had a mass of 16 g. The oxygen content determined by thermogravimetric analysis of a specimen from the same boule was $\delta=0.11\pm0.01$.

Neutron scattering measurements were made on the MAPS time-of-flight spectrometer at ISIS and on the IN8 and IN20 triple-axis spectrometers at the ILL. A preliminary report of the MAPS data has already been published.[31] On MAPS, the crystal was aligned with the c axis parallel to the incident beam direction. Spectra were recorded with several incident neutron energies, and the scattering from a standard vanadium sample was used to normalize the spectra and place them on an absolute intensity scale. On IN8 and IN20, the crystal was mounted with the c axis and [110] direction in the horizontal scattering plane (we refer throughout to the tetragonal unit cell with lattice parameters $a=3.85$ Å and $c=12.7$ Å), and the spectrometers were configured for a fixed final neutron energy of $E_f=14.7$ meV with a graphite filter after the sample to suppress higher orders.

Measurements on IN20 employed uniaxial polarization analysis.[32] Polarized neutron diffraction (elastic scattering) data were collected with three orthogonal orientations of **P** relative to **Q**: (1) $\mathbf{P}\|\mathbf{Q}$, (2) $\mathbf{P}\perp\mathbf{Q}$ with **P** in the scattering plane, and (3) $\mathbf{P}\perp\mathbf{Q}$ with **P** perpendicular to the scattering plane. The data were used to probe the spin orientation in the magnetically ordered phase. The spin-flip (SF) and non-spin-flip (NSF) components of two magnetic Bragg peaks were measured for each of the three orthogonal directions of **P**. Corrections were applied to compensate for the imperfect neutron polarization. For the inelastic scattering measurements the neutron spin polarization **P** was maintained parallel to the scattering vector **Q** in order to separate magnetic from nonmagnetic scattering

III. RESULTS

Neutron diffraction measurements revealed patterns consistent with diagonal stripe order (i.e., stripes oriented at 45° to the Ni–O bonds) characterized by a fourfold group of magnetic diffraction peaks at IC wave vectors $\mathbf{Q}_{IC}=\mathbf{Q}_{AF}\pm(\epsilon/2,\epsilon/2,0)$ and $\mathbf{Q}_{AF}\pm(-\epsilon/2,\epsilon/2,0)$, where h, k, and l are integers, $\mathbf{Q}_{AF}=(h+0.5,k+0.5,l)$ are antiferromagnetic wave vectors, and $\epsilon=0.270\pm0.005$ is the incommensurability.[33] These peaks were observed below $T_N\simeq120$ K, consistent with previous data.[23,24] The observation of four satellites around $\mathbf{Q}_{AF}$ is explained by the presence of domains in which the charge stripes run along the two equivalent diagonals of the square lattice, as shown schematically in Fig. 1 for ideal period-4 stripes. The domain with stripes parallel to the $[1\bar{1}0]$ direction gives rise to the magnetic peaks displaced by $\pm(\epsilon/2,\epsilon/2,0)$ from $\mathbf{Q}_{AF}$, while the [110] stripe domain causes the peaks displaced by $\pm(-\epsilon/2,\epsilon/2,0)$ from $\mathbf{Q}_{AF}$. The correlation lengths for the magnetic order were found to be ~50 Å both parallel and perpendicular to the stripes in the ab plane, and ~90 Å in the c direction. We also observed the distinct sets of superlattice peaks associated with interstitial oxygen ordering reported in Ref. 34.

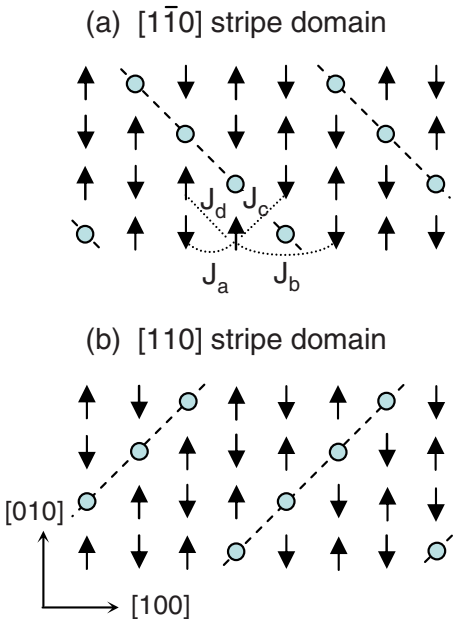

FIG. 1. (Color online) Model for ideal period-4 diagonal stripes (DS4 model). Two equivalent domains are shown, with stripes running parallel to the (a) $[1\bar{1}0]$ and (b) [110] directions of the square lattice. In relation to hole-doped nickelates, the arrows show AFM ordered spins on Ni^{2+} sites and the filled circles represent doped holes assumed here to be localized on Ni^{3+} ions. Exchange interactions considered in the spin-wave analysis are indicated.

The polarized neutron diffraction measurements depend on the Fourier component $\mathbf{M}(\mathbf{Q})$ of the magnetic structure at the ordering wave vector $\mathbf{Q}=\mathbf{Q}_{IC}$. Following the approach described in Ref. 35, we used the six measurements (SF and NSF components for three orientations of **P** relative to **Q**) at the magnetic Bragg peaks $\mathbf{Q}_1=(0.5-\epsilon/2,0.5-\epsilon/2,3)$ and $\mathbf{Q}_2=(0.5+\epsilon/2,0.5+\epsilon/2,1)$ to determine the intensities associated with the components of $\mathbf{M}(\mathbf{Q}_{IC})$ along the [110], $[1\bar{1}0]$, and [001] directions. The data collected at 2 K gave $I_{110}/I_{1\bar{1}0}=0.062\pm0.004$ and $I_{001}/(I_{110}+I_{1\bar{1}0})=0.004\pm0.004$. Within experimental error these ratios did not vary with temperature between 2 and 60 K. For collinear magnetic order $\mathbf{M}(\mathbf{Q})$ is proportional to the ordered moment, and assuming this to be the case here we find that the ordered moments lie in the ab plane to within an experimental uncertainty of 5° and make an in-plane angle of $14.0\pm0.5°$ to the stripe direction.

We now turn to the magnetic excitation spectrum. Figures 2(a)–2(c) show constant-energy slices that illustrate the most notable features of the observed spectrum. The data, which were recorded on MAPS with unpolarized neutrons of incident energy 80 meV and a sample temperature of 7 K, have been averaged over the indicated energy ranges and plotted as a function of the in-plane scattering vector $\mathbf{Q}_{2D}=(h,k)$ in reciprocal lattice units (r.l.u.).[36] The 7–9 meV slice exhibits four peaks at the magnetic ordering wave vectors. The intensities of the peaks are unequal because the ordered moments make different angles to **Q** in the two stripe domains.[37]

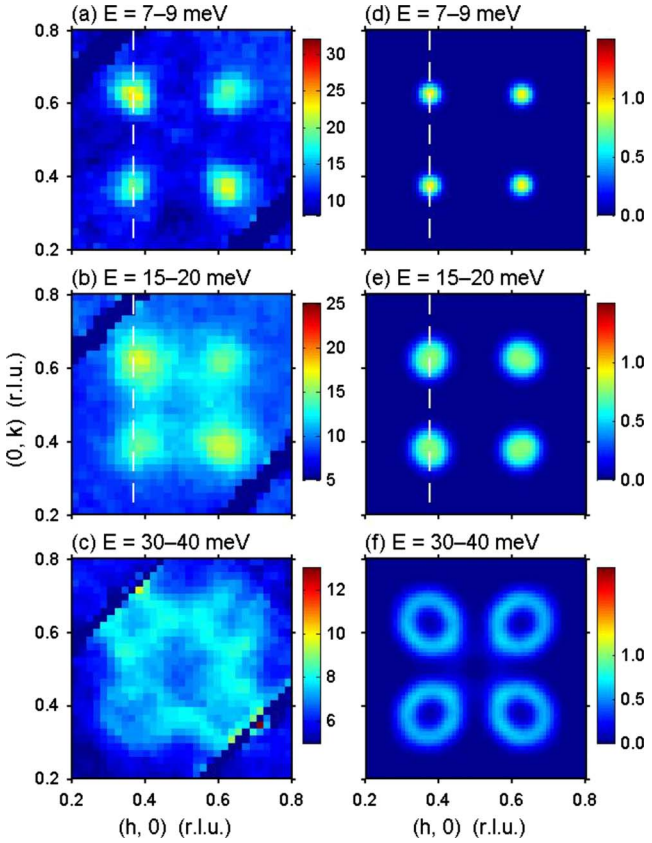

FIG. 2. (Color online) Spin excitation spectrum of $La_2NiO_{4.11}$ measured by inelastic neutron scattering and calculated by linear spin-wave theory. (a)–(c) Constant-energy slices averaged over the energy ranges indicated above the figures. Vertical dashes mark the positions of maximum intensity in the 7–9 meV slices. The data were collected on the MAPS spectrometer with a sample temperature of 7 K and with incident neutron energies of 80 meV. The intensity is in units of mb sr^{-1} meV^{-1} f.u.$^{-1}$, where f.u. stands for "formula unit" (of $La_2NiO_{4.11}$). (e)–(g) Simulations based on the DS4 model shown in Fig. 1 (Ref. 39) with exchange constants J_a =28 meV, J_b=17 meV and J_c=J_d=0 meV, and 2D Gaussian wave vector broadening with standard deviation 0.022 r.l.u. The intensity in the simulations is in arbitrary units.

These four peaks are also present in the 15–20 meV slice but have clearly shifted inwards toward $\mathbf{Q}_{AF}$=(0.5,0.5). Above 25 meV these peaks evolve into rings as can be seen in the 30–40 meV slice. The features just described are significantly broader in wave vector than the experimental resolution, which is approximately 0.05 r.l.u under the conditions used to collect the data in Figs. 2(a)–2(c). Above ~50 meV the rings strongly overlap and merge into a single broad peak centered on $\mathbf{Q}_{AF}$. As shown in Fig. 3, the peak at $\mathbf{Q}_{AF}$ decreases in intensity with increasing energy up to ~110 meV, above which no signal can be detected above the background.

We performed additional measurements with neutron polarization analysis to distinguish magnetic from nonmagnetic scattering. Figure 4 (main panel) shows a series of constant-energy scans along the (ξ,ξ) direction measured on IN20 in the spin-flip scattering channel. With $\mathbf{P}\|\mathbf{Q}$ the SF scattering is purely magnetic. Up to 10 meV, the scans show peaks

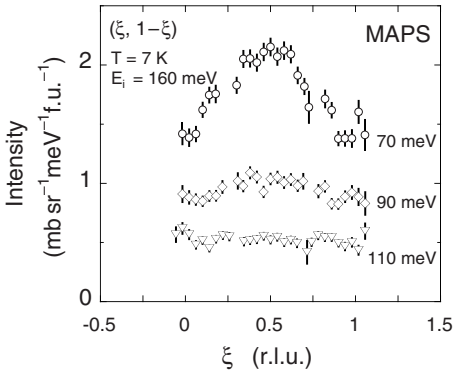

FIG. 3. Constant-energy cuts through the excitation spectrum of $La_2NiO_{4.11}$ parallel to the $(\xi,-\xi)$ direction through (0.5, 0.5). No offset has been applied to the scans at different energies.

centered at the same wave vectors as the magnetic Bragg peaks, which are also shown in the figure, but above 10 meV the peaks move inwards and broaden compared with the resolution. Interestingly, even at 10 meV the peaks are about 50% broader than the experimental resolution.

These results confirm that the inward-dispersing peaks found here are magnetic in origin. The upper panel of Fig. 4 shows a cut through the MAPS data along the direction perpendicular to the stripes, averaged over the energy range 45–50 meV. This illustrates the splitting of the IC peaks at higher energies [see also Fig. 2(c)].

To quantify the dispersion, we fitted Lorentzian functions to the peaks in a series of constant-energy scans including those shown in Fig. 4. The fitted peak centers are plotted in Fig. 5. Data from all three spectrometers are included in the analysis and are consistent with one another. One can see clearly how the peak intensity remains centered at the magnetic ordering wave vectors up to 10 meV, above which it disperses inwards. At 20 meV the incommensurability is 20–25% less than the static value. This analysis confirms that the shift observable in the raw intensity data is intrinsic and not simply an artifact from the overlap of the peaks. Above 25 meV, four peaks can be resolved in the scans and the data were accordingly fitted to four Lorentzian functions. The resulting pair of "*V*"-shaped dispersion curves are asymmetric, with higher velocity on the inner branches. This asymmetry partially counteracts the inward shift in intensity at lower energies, but even in the highest energy data (45–50 meV) the pairs of spin-wave peaks are still shifted toward $\mathbf{Q}_{AF}$ relative to the magnetic Bragg peaks.

An obvious question to ask now is, do other stripe-ordered nickelates exhibit similar features to those just described? The question is answered for one other composition in Fig. 6. This figure shows the magnetic dispersion of $La_{5/3}Sr_{1/3}NiO_4$, which has commensurate period-3 charge stripes (ϵ=1/3). The dispersion was obtained from a series of constant-energy cuts along the (ξ,ξ) direction through the MAPS data set of Woo *et al.*[29] As before, a two- or four-Lorentzian line shape was used to obtain the peak positions. To within experimental error the dispersion is symmetric about the magnetic Bragg peak positions, in stark contrast to the case of $La_2NiO_{4.11}$.

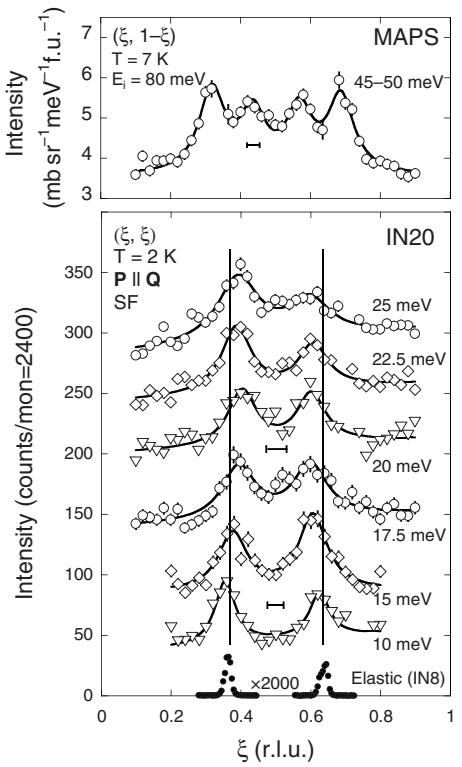

FIG. 4. Constant-energy scans through the spin excitation spectrum of $La_2NiO_{4.11}$ in the direction perpendicular to the stripes. The inelastic data in the lower panel were recorded on IN20 employing neutron polarization analysis. The spin-flip (SF) channel contains purely magnetic scattering. Vertical lines mark the positions of the magnetic Bragg peaks, shown at the base of the frame. The scans were measured in several different zones: $(\xi,\xi,4)$ for 10 and 15 meV, $(\xi+1,\xi+1,0)$ for 17.5, 20, and 25 meV, and $(\xi+1,\xi+1,0.5)$ for 22.5 meV. Each scan is offset vertically by 50 counts. The solid lines are the results of fits to two Lorentzian functions with equal widths. The upper panel shows a cut through the MAPS data averaged over the energy range 45–50 meV. The out-of-plane wave vector is $l \simeq 5$. The solid line is a fit to four Lorentzians with equal peak widths. Horizontal bars in both panels indicate the wave vector resolution.

IV. ANALYSIS AND DISCUSSION

The data presented in the previous section show conclusively that there is an inward shift toward $\mathbf{Q}_{AF}$ in the intensity of the spin excitation spectrum of $La_2NiO_{4.11}$ for energies above ~ 10 meV, whereas there is no such shift for the commensurate stripe-ordered compound $La_{5/3}Sr_{1/3}NiO_4$. Since the spins in the stripe phase are localized and ordered the dominant magnetic excitations are expected to be spin precession waves, so a natural first step is to see whether the results can be understood in the framework of linear spin-wave theory.

Linear spin-wave theory (LSWT) has been used previously to investigate the spin excitation spectrum of ideal commensurate stripe structures.[38,39] The calculations assume a Heisenberg spin Hamiltonian, so charge dynamics are included only insofar as they modify the strength of the interstripe exchange couplings. To test whether LSWT can describe the anomalous features of the spin excitation spectrum of $La_2NiO_{4.11}$, we compared the data with LSWT predictions for ideal site-centered period-4 diagonal charge stripes as shown in Fig. 1, dubbed DS4 in Ref. 39, for which the incommensurability $\epsilon=0.25$ is close to that observed experimentally ($\epsilon \simeq 0.27$). The minimal DS4 model has two exchange parameters, one (J_a) coupling nearest-neighbor Ni^{2+} spins within a stripe domain, and the other (J_b) coupling Ni^{2+} spins either side of a domain wall in a straight line through a Ni^{3+} site. The justification for this model is that it provides a very good description of the magnetic dispersion of $La_{5/3}Sr_{1/3}NiO_4$.[27,29]

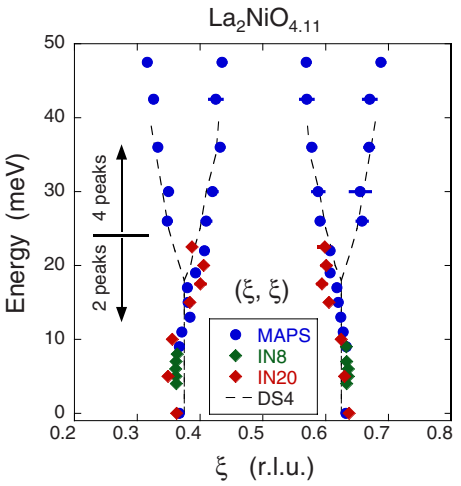

FIG. 5. (Color online) Dispersion of magnetic excitations in $La_2NiO_{4.11}$. Data points are peak centers from fits to a series of constant-energy scans made on MAPS, IN20, and IN8. Data below (above) 25 meV were fitted to two (four) Lorentzian functions on a linear background. The broken lines show the peak positions from the LSWT simulations for the DS4 model (Fig. 1).

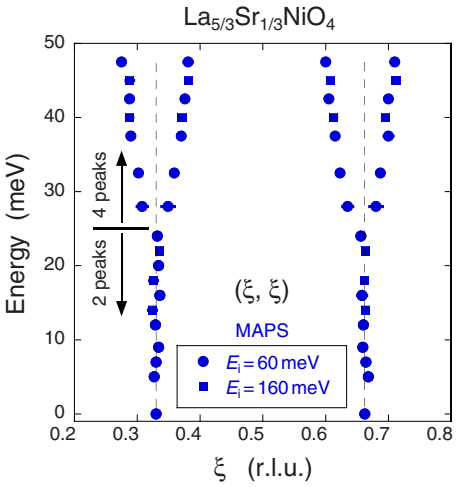

FIG. 6. (Color online) Dispersion of magnetic excitations in $La_{5/3}Sr_{1/3}NiO_4$. The data are from the study by Woo *et al.* (Ref. 29). Points are peak centers from fits to a series of constant-energy scans made on MAPS with incident energies of 60 and 160 meV. Data below (above) 25 meV were fitted to two (four) Lorentzian functions on a linear background. The broken lines mark the magnetic Bragg peak positions.

A detailed comparison with the model is not possible because the experimental spectrum of $La_2NiO_{4.11}$ has considerable intrinsic broadening and at high energies is complicated by the twinning of the stripes. Instead, we estimate the parameters of the model as follows. The magnetic dispersion of the J_a-J_b DS4 model has a band width of $4J_a$ (we assume $S=1$). The experimental magnon bandwidth is 110 ± 10 meV, so $J_a=28\pm3$ meV. To estimate J_b, we fitted the slope of the acoustic magnon branch perpendicular to the stripes to the data above 25 meV in Fig. 5. This gave $J_b=17\pm3$ meV. The values of J_a and J_b agree closely with those determined experimentally for $La_{5/3}Sr_{1/3}NiO_4$ ($J_a=27.5\pm0.4$ meV, $J_b=13.6\pm0.3$ meV) (Refs. 27 and 29) and J_a is in good agreement with that obtained for La_2NiO_4 ($J_a=31\pm0.7$ meV).[40]

Figures 2(d)–2(f) show simulated constant-energy slices from the J_a-J_b DS4 model alongside the corresponding data from MAPS. The simulations reproduce most features of the data but, crucially, they do not exhibit the inward dispersion of the incommensurate peaks.

It has been shown that an apparent inward dispersion can be obtained for striped spin structures within LSWT when $J_b \ll J_a$.[18] In this case, the inward dispersion is the combined effect of broadening and a stronger intensity on the surface of the spin-wave cone nearest $\mathbf{Q}_{AF}$. A reduction in J_b/J_a is only possible within the constraints imposed by the $La_2NiO_{4.11}$ data if we introduce additional exchange parameters. However, the inclusion of diagonal next-nearest-neighbor Ni–Ni couplings between (J_c) and within (J_d) stripe domains did not enable us to reproduce the observed 20–25% inwards intensity shift within the DS4 model without departing from the observed magnon bandwidth of ~110 meV and/or the data shown in Fig. 5. We also performed simulations for period-4 bond-centered stripes, but we could not reproduce the inwards intensity shift with this model either.

Our results suggest that the magnetic dynamics of $La_2NiO_{4.11}$ require a description beyond the simplest LSWT of ideal stripes. Some of the following features may be needed: first, the stripes in $La_2NiO_{4.11}$ are not commensurate but have a period slightly less than four lattice spacings. A mixture of ~25% period-3 stripes and ~75% period-4 stripes is expected, and irregularities in the arrangement may explain the observed broadening of the spin waves. Second, $La_2NiO_{4.11}$ is close to the border between stripe order and La_2NiO_4-like AFM order.[23,24] Competition between these order parameters may influence the magnetic spectrum. Third, coupling between spin and charge degrees of freedom has so far been neglected. Finally, we recall that an as-yet unexplained resonance/gaplike feature appears in the magnetic spectrum of $La_{2-x}Sr_xNiO_4$ with $x\sim1/3$ (Refs. 27 and 28) in the same energy range as the observed inward dispersion in $La_2NiO_{4.11}$. It is possible that these anomalous features are related.

V. CONCLUSION

This work was motivated by the possibility that charge-stripe correlations might be behind the hour-glass magnetic spectrum found in the hole-doped cuprates. Our results show that one feature of the cuprate spectrum, namely, the inward dispersion at low energies, is also found in an insulating nickelate with well-correlated but incommensurate stripe order. This similarity is intriguing, but does not necessarily imply that the inward magnetic dispersion has a common origin in the two systems since there are important differences between hole-doped cuprates and nickelates. Nevertheless, our results do emphasize that the magnetic spectra of stripe-ordered materials contain interesting features that need to be understood better. Attempts to understand the inward dispersion in the particular case of $La_2NiO_{4.11}$ will need to go beyond the simplest model of ideal period-4 stripes used here.

ACKNOWLEDGMENTS

A.T.B. is grateful to the Laboratory for Neutron Science at the Paul Scherrer Institute for hospitality and support during an extended visit in 2009. This work was supported by the Engineering & Physical Sciences Research Council of Great Britain, Research Corporation, and U.S. NSF under Grant No. DMR 08-04748.

*a.boothroyd@physics.ox.ac.uk

[1] M. Vojta, Adv. Phys. **58**, 564 (2009).
[2] M. Arai, T. Nishijima, Y. Endoh, T. Egami, S. Tajima, K. Tomimoto, Y. Shiohara, M. Takahashi, A. Garrett, and S. M. Bennington, Phys. Rev. Lett. **83**, 608 (1999).
[3] P. Bourges, Y. Sidis, H. F. Fong, L. P. Regnault, J. Bossy, A. Ivanov, and B. Keimer, Science **288**, 1234 (2000).
[4] S. M. Hayden, H. A. Mook, P. C. Dai, T. G. Perring, and F. Dogan, Nature (London) **429**, 531 (2004).
[5] J. M. Tranquada, H. Woo, T. G. Perring, H. Goka, G. D. Gu, G. Xu, M. Fujita, and K. Yamada, Nature (London) **429**, 534 (2004).
[6] N. B. Christensen, D. F. McMorrow, H. M. Rønnow, B. Lake, S. M. Hayden, G. Aeppli, T. G. Perring, M. Mangkorntong, M. Nohara, and H. Takagi, Phys. Rev. Lett. **93**, 147002 (2004).
[7] D. Reznik, P. Bourges, L. Pintschovius, Y. Endoh, Y. Sidis, T. Masui, and S. Tajima, Phys. Rev. Lett. **93**, 207003 (2004).
[8] C. Stock, W. J. L. Buyers, R. A. Cowley, P. S. Clegg, R. Coldea, C. D. Frost, R. Liang, D. Peets, D. Bonn, W. N. Hardy, and R. J. Birgeneau, Phys. Rev. B **71**, 024522 (2005).
[9] B. Vignolle, S. M. Hayden, D. F. McMorrow, H. M. Rønnow, B. Lake, C. D. Frost, and T. G. Perring, Nat. Phys. **3**, 163 (2007).
[10] V. Hinkov, P. Bourges, S. Pailhès, Y. Sidis, A. Ivanov, C. D. Frost, T. G. Perring, C. T. Lin, D. P. Chen, and B. Keimer, Nat. Phys. **3**, 780 (2007).
[11] M. Matsuda, M. Fujita, S. Wakimoto, J. A. Fernandez-Baca, J. M. Tranquada, and K. Yamada, Phys. Rev. Lett. **101**, 197001 (2008).

[12] J. M. Tranquada, B. J. Sternleib, J. D. Axe, Y. Nakamura, and S. Uchida, Nature (London) **375**, 561 (1995).
[13] C. D. Batista, G. Ortiz, and A. V. Balatsky, Phys. Rev. B **64**, 172508 (2001).
[14] M. Vojta and T. Ulbricht, Phys. Rev. Lett. **93**, 127002 (2004).
[15] G. S. Uhrig, K. P. Schmidt, and M. Grüninger, Phys. Rev. Lett. **93**, 267003 (2004).
[16] G. Seibold and J. Lorenzana, Phys. Rev. Lett. **94**, 107006 (2005).
[17] B. M. Andersen and P. Hedegård, Phys. Rev. Lett. **95**, 037002 (2005).
[18] D. X. Yao, E. W. Carlson, and D. K. Campbell, Phys. Rev. Lett. **97**, 017003 (2006).
[19] See, however, Ref. 18.
[20] S. M. Hayden, G. H. Lander, J. Zarestky, P. J. Brown, C. Stassis, P. Metcalf, and J. M. Honig, Phys. Rev. Lett. **68**, 1061 (1992).
[21] C. H. Chen, S.-W. Cheong, and A. S. Cooper, Phys. Rev. Lett. **71**, 2461 (1993).
[22] J. M. Tranquada, D. J. Buttrey, V. Sachan, and J. E. Lorenzo, Phys. Rev. Lett. **73**, 1003 (1994).
[23] K. Yamada, T. Omata, K. Nakajima, Y. Endoh, and S. Hosoya, Physica C **221**, 355 (1994).
[24] J. M. Tranquada, Y. Kong, J. E. Lorenzo, D. J. Buttrey, D. E. Rice, and V. Sachan, Phys. Rev. B **50**, 6340 (1994).
[25] H. Yoshizawa, T. Kakeshita, R. Kajimoto, T. Tanabe, T. Katsufuji, and Y. Tokura, Phys. Rev. B **61**, R854 (2000).
[26] P. Bourges, Y. Sidis, M. Braden, K. Nakajima, and J. M. Tranquada, Phys. Rev. Lett. **90**, 147202 (2003).
[27] A. T. Boothroyd, D. Prabhakaran, P. G. Freeman, S. J. S. Lister, M. Enderle, A. Hiess, and J. Kulda, Phys. Rev. B **67**, 100407(R) (2003).
[28] A. T. Boothroyd, P. G. Freeman, D. Prabhakaran, M. Enderle, and J. Kulda, Physica B **345**, 1 (2004).
[29] H. Woo, A. T. Boothroyd, K. Nakajima, T. G. Perring, C. D. Frost, P. G. Freeman, D. Prabhakaran, K. Yamada, and J. M. Tranquada, Phys. Rev. B **72**, 064437 (2005).
[30] D. Prabhakaran, P. Isla, and A. T. Boothroyd, J. Cryst. Growth **237-239**, 815 (2002).
[31] P. G. Freeman, S. M. Hayden, C. D. Frost, D. Prabhakaran, and A. T. Boothroyd, J. Magn. Magn. Mater. **310**, 760 (2007).
[32] R. M. Moon, T. Riste, and W. C. Koehler, Phys. Rev. **181**, 920 (1969).
[33] When $\epsilon=0.25$, stripes are commensurate with period 4.
[34] J. M. Tranquada, J. E. Lorenzo, D. J. Buttrey, and V. Sachan, Phys. Rev. B **52**, 3581 (1995).
[35] P. G. Freeman, A. T. Boothroyd, D. Prabhakaran, D. González, and M. Enderle, Phys. Rev. B **66**, 212405 (2002).
[36] Note that in the time-of-flight method the out-of-plane component of the scattering vector (l) varies with energy and across the detector. However, the spin dynamics of $La_2NiO_{4.11}$ are highly two-dimensional and so the l variation only affects the intensity and not the dispersion. We have confirmed this by performing an l scan through $\mathbf{Q}_{AF}$ at a fixed energy of 8 meV. The scan showed no periodic modulation in the intensity with l.
[37] Inelastic neutron scattering probes spin fluctuations perpendicular to $\mathbf{Q}$. For a collinear magnet with isotropic transverse spin fluctuations the intensity is proportional to the factor $g(\theta)=\langle 1+\cos^2\theta\rangle$, where θ is the angle between the ordered moments and $\mathbf{Q}$, and the average is taken over equivalent spin orientation domains. The difference in $g(\theta)$ for the two stripe domains explains why the magnetic scattering from one stripe domain is more intense than that from the other. For example, for the $E=7-9$ meV slice [Fig. 2(a)], assuming the moments to be at 14° to the stripe direction, we find $g(\theta)\simeq 1.1$ for the $[1\bar{1}0]$ stripe domain and $g(\theta)\simeq 1.7$ for the [110] stripe domain. Therefore, assuming equal populations of the two stripe domains we find that the magnetic peaks associated with the [110] stripe domain should be more intense than those associated with the $[1\bar{1}0]$ stripe domain. This is consistent with the data in Fig. 2(a).
[38] F. Krüger and S. Scheidl, Phys. Rev. B **67**, 134512 (2003).
[39] E. W. Carlson, D. X. Yao, and D. K. Campbell, Phys. Rev. B **70**, 064505 (2004).
[40] K. Nakajima, K. Yamada, S. Hosoya, T. Omata, and Y. Endoh, J. Phys. Soc. Jpn. **62**, 4438 (1993).